COMPDYN 2011
III ECCOMAS Thematic Conference on
Computational Methods in Structural Dynamics and Earthquake Engineering
M. Papadrakakis, M. Fragiadakis, V. Plevris (eds.)
Corfu, Greece, 25–28 May 2011

DEVELOPMENT OF A FAMILY OF UNCONDITIONALLY STABLE EXPLICIT DIRECT INTEGRATION ALGORITHMS WITH CONTROLLABLE NUMERICAL DAMPING USING DISCRETE CONTROL THEORY

Cheng Chen[1], **and James M. Ricles**[2]

[1] School of Engineering, San Francisco State University
San Francisco, CA 94132
e-mail: chcsfsu@sfsu.edu

[2] Department of Civil and Environmental Engineering, Lehigh University
Bethlehem, PA 94132
jmr5@lehigh.edu

Keywords: Numerical Algorithm, Control Theory, Stability, Structural Dynamics, Numerical Damping.

Abstract. *Integration algorithms are typically utilized to solve temporally discretized equations of motion in structural dynamics. Stability is an important property to be considered when selecting the proper integration algorithm for analysis of structures with a large number of degrees of freedom. The recent development of real-time structural testing brings more challenges to the integration algorithm. An explicit integration algorithm is more favorable in real-time structural testing because of its computational efficiency. However, the presence of numerical errors will lead to the spurious growth of high-frequency response in the dynamic analysis and the presence of inevitable experimental errors will aggravate this effect during real-time structural testing. It is therefore advantageous for an explicit integration algorithm to possess numerical damping to suppress any spurious participation of the high-frequency response while the lower modes are accurately integrated. This paper presents the development of a family of explicit direct integration algorithms with controllable numerical damping. Discrete control theory is utilized to assign proper stable poles to the discrete transfer function of the integrations algorithms to achieve unconditional stability and numerical damping. The properties of the proposed algorithm are investigated and compared with other well established algorithms such as the Newmark family of integration algorithms and the CR integration algorithm.*

1 INTRODUCTION

Integration algorithms are usually utilized to solve the equations of motion of structures subjected to external excitations. Various integration algorithms have been developed and applied in structural dynamics such as the Newmark Family of integration algorithms [1] and the Hilber-Hughes-Taylor α-method [2]. Various methods have been used to develop integration algorithms, including Taylor series expansions, weighted residual methods, Hamilton's principle, and least-squares methods [3]. Currently available integration algorithms can usually be classified as either explicit or implicit. An integration algorithm is explicit if the displacements for the next time step can be determined from the accelerations, velocities and displacements at the current and previous time step, otherwise it is implicit. The implicit integration algorithms are usually unconditionally stable such as the Newmark method with constant average acceleration and the HHT α-method, while the explicit integration algorithms are often conditionally stable, including the Newmark explicit method and the central difference method. In many structural dynamics applications, where iterations are not concerned in the analysis, the implicit integration algorithms with unconditional stability are generally preferred over conditionally stable explicit integration algorithms.

In addition to the structural dynamic analysis, integration algorithms are also applied in online structural experiments, where they are utilized to solve the dynamics of a prototype structure to sequentially determine the displacement response of an experimental structure in the laboratory. This application was first investigated by Takanashi *et al.* [4] and then by Mahin and Shing [5], and can be categorized as quasi-static pseudodynamic testing or quasi-static substructure testing. It is believed that by having the structural components (usually difficult to model numerically) tested in the laboratory and keeping the remainder of the structural system modeled analytically, the response of the entire structure under a selected ground motion can be replicated in an economic and efficient manner. Both explicit and implicit integration algorithms have been utilized in quasi-static pseudodynamic and substructure testing [5, 6]. Since the experiments are conducted in an extended time scale (i.e., quasi-statically), the required iterations for implicit integration algorithms are not critical and the implicit integration algorithms therefore are often used because of their unconditional stability.

Recent earthquake engineering research have advanced the quasi-static pseudodynamic and substructures testing methods to real-time pseudodynamic testing [7] and real-time hybrid simulation [8] to accommodate rate-dependent behavior in the experimental specimens. These two structural testing methods will be referred to as real-time testing hereafter. Unlike the conventional experimental methods, real-time testing requires that the command displacements from the integration algorithm be applied accurately to the experimental substructures in a real-time manner. Integration algorithms therefore are required to solve the equations of motion and compute the command displacements in a timely manner so as not to introduce any time delay in the real-time test. This poses a great challenge to the integration algorithm when the real-time test involves a complex structure with a large number of degrees of freedom. Explicit integration algorithms thus present more attractive solution for real-time testing than implicit integration algorithms since no iterations are necessary.

More recently, several unconditionally stable explicit integration algorithms were developed by researchers to enable real-time structural tests [9, 10]. Unlike other available integration algorithms, integration parameters of these algorithms are defined as functions of the linear elastic properties of the structure to be analyzed. By carefully selecting the integration parameters, these algorithms possess both explicitness and unconditional stability. When applied for nonlinear structural behavior, Chen and Ricles [11, 12] showed that these algorithms maintain the stability when the structure has softening behavior. The explicitness and uncon-

ditional stability of these integration algorithm present great potential for real-time structural testing. Chen *et al.* [13] implemented the unconditional explicit CR integration algorithm for real-time hybrid simulation of structures with an elastomeric damper. The experiment results were compared with those using the existing HHT α-method with a fixed number of substep iteration [14]. Good agreement was observed, indicating that the unconditional explicit CR algorithm is applicable for real-time testing. Chen *et al.* [15] further extended the application of the CR algorithm for the real-time hybrid simulation of a moment resisting frame (MRF) with magneto-rheological (MR) dampers in passive mode. The prototype MRF had a total of 122 degrees of freedom and 71 elements. The experimental results was later compared with pure numerical simulation by Chen *et al.* [16]. Good agreement further validated the effectiveness of the CR algorithm for real-time testing. However, it was observed that the experimental results, especially the restoring forces in the experimental substructures (i.e., the MR dampers), had high frequency noise. Small oscillation was also observed in the structural displacement response. These high frequency mode responses are attributed to the spatially discretized equations of motion and do not necessarily represent the true behavior of the prototype structure under earthquakes. In addition, the presence of numerical errors will lead to the spurious growth of high-frequency response and the inevitable experimental errors will aggravate this effect in real-time tests. Therefore, it is advantageous for an algorithm to possess numerical damping to suppress any spurious participation of the high-frequency response and minimize the effect of numerical and experimental errors, while the lower modes can be integrated accurately. However, the current unconditionally stable explicit CR integration algorithm has zero or only little numerical damping properties. It is thus desirable to introduce controllable numerical damping into the algorithm while maintaining its explicitness and unconditional stability. This paper presents the development of a family of unconditionally stable explicit integration algorithm using the discrete control theory.

2 INTEGRATION ALGORITHM AND DISCRETE TRANSFER FUNCTION FOR SDOF STRUCTURE

Consider a single-degree-of-freedom (SDOF) linear elastic structure represented by the following differential equation of motion under external excitation $F(t)$:

$$m \cdot \ddot{x}(\mathrm{t}) + c \cdot \dot{x}(\mathrm{t}) + k \cdot x(t) = F(t) \tag{1a}$$

where m, c and k are the mass, viscous damping and linear elastic stiffness of the SDOF structure, respectively; and $x(t)$, $\dot{x}(t)$, $\ddot{x}(t)$ are the displacement, velocity and acceleration of the SDOF structure, respectively. Integration algorithms in structural dynamics are usually applied to solve the temporally discretized equation of motion of Eq. (1a) for structural response, which can be written as:

$$m \cdot \ddot{x}_{\mathrm{i}+1} + c \cdot \dot{x}_{\mathrm{i}+1} + k \cdot x_{\mathrm{i}+1} = F_{\mathrm{i}+1} \tag{1b}$$

where x_{i+1}, $\dot{x}_{i+1}$, $\ddot{x}_{i+1}$ are the displacement, velocity and acceleration of the SDOF structure at the $(i+1)^{\mathrm{th}}$ time step, respectively; and $F_{\mathrm{i}+1}$ is the value of excitation $F(t)$ at the $(i+1)^{\mathrm{th}}$ time step.

To obtain an explicit integration algorithm, the variation of the displacement and velocity over the time step can be defined as

$$\dot{x}_{\mathrm{i}+1} = \dot{x}_{\mathrm{i}} + \alpha_1 \cdot \Delta t \cdot \ddot{x}_{\mathrm{i}} \tag{2a}$$

$$x_{i+1} = x_i + \Delta t \cdot \dot{x}_{\mathrm{i}} + \alpha_2 \cdot \Delta t^2 \cdot \ddot{x}_{\mathrm{i}} \tag{2b}$$

where α_1 and α_2 are integration parameters and will be determined later; x_i, $\dot{x}_i$, $\ddot{x}_i$ are the displacement, velocity and acceleration of the SDOF structure at the i^{th} time step, respectively; and Δt is the time step for the dynamic analysis.

It can be observed that both the displacement x_{i+1} and velocity $\dot{x}_{i+1}$ in Eqs. (2a) and 2(b) are explicit since they are only dependent on the structural response of the previous time step. This explicitness will lead to significant computational efficiency when the algorithm is used in dynamic analysis structures subjected to earthquakes. Eqs. (2a) and (2b) were also used by Chen and Ricles [10] to develop the unconditionally stable CR explicit integration algorithm. The discrete transfer function G(z) for the integration algorithms can be derived by substituting Eqs. (2a) and (2b) into Eq. (1b), whereby it can be written in the following general form

$$G(z) = \frac{X(z)}{F(z)} = \frac{n_2 z^2 + n_1 z + n_0}{d_2 z^2 + d_1 z + d_0} \tag{3}$$

where $G(z)$ is a discrete transfer function relating the displacement response of the structure and the external excitation; $X(z)$ and $F(z)$ are discrete z-transforms of the displacement response x_{i+1} and excitation force F_{i+1}, respectively; z is the complex variable in the discrete z-domain; n_2, n_1, n_0, d_2, d_1 and d_0 are coefficients of the numerator and denominator of the discrete transfer function $G(z)$, respectively. The coefficients of the discrete transfer function are tabulated in Table 1 for the new algorithms. It can be observed that the coefficients in Table 1 are dependent on the structure properties (m, c, and k) and the integration time step Δt as well as the two integration parameters (α_1 and α_2).

Numerator		Denominator	
n_2	0	d_2	m
n_1	$\alpha_2 \cdot \Delta t^2$	d_1	$\alpha_2 \cdot k \cdot \Delta t^2 + \alpha_1 \cdot c \cdot \Delta t - 2m$
n_0	$(\alpha_1 - \alpha_2) \cdot \Delta t^2$	d_0	$(\alpha_1 - \alpha_2) \cdot k \cdot \Delta t^2 - \alpha_1 \cdot c \cdot \Delta t + m$

Table 1. Coefficients of G(z) for the new integration algorithm

Chen and Ricles [10] indicated that the poles of the discrete transfer function $G(z)$ in Eq. (3) determine the properties of the corresponding integration algorithm including the stability and accuracy. The complex poles of $G(z)$ in Eq. (3) can be written in the following form

$$p_{1,2} = \sigma \pm \varepsilon \cdot i = \exp[\overline{\Omega} \cdot (-\zeta_{eq} \pm i\sqrt{1-\zeta_{eq}^2})] \tag{4}$$

where σ and ε are the real components, and i is the imaginary unit defined as $i = \sqrt{-1}$; the apparent frequency $\overline{\Omega}$ and the equivalent damping ratio ζ_{eq} are defined as

$$\overline{\Omega} = \tan^{-1}(\varepsilon / \sigma) / (\sqrt{1-\zeta_{eq}^2}) \tag{5a}$$

$$\zeta_{eq} = -\ln\left(\sigma^2 + \varepsilon^2\right) / 2\overline{\Omega} \tag{5b}$$

The integration algorithm will be unconditionally stable if the poles in Eq. (4) are always located inside or on the unit circle of the discrete z-domain as shown in Figure 1. Otherwise, the algorithm is conditionally stable. Compared with the conventional stability criterion [17], the magnitude of the complex poles in Eq. (4) represent the spectral radius, while Eqs. (5a) and (5b) determine the period elongation and numerical damping of the integration algorithm.

To achieve unconditional stability, Chen and Ricles [10] used the Tustin transform [18] to discretize the continuous poles and assigned the resulting discrete poles to the discrete transfer function in Eq. (3), which leads to the integration parameters α_1 and α_2 for the unconditionally stable explicit CR algorithm.

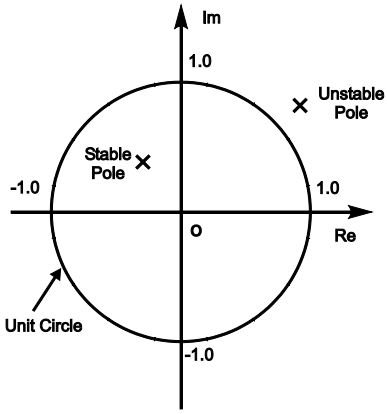

Figure 1: Schematic of Stable and Unstable Poles in Complex z-domain.

3 INTEGRATION PARAMETER DERIVATION FOR INTEGRATION ALGORITHMS WITH NUMERICAL DAMPING

Chen and Ricles [11, 12] demonstrated that an integration algorithm can schematically be represented by a open-loop block diagram in Figure 2(a), or by a closed-loop block diagram in Figure 2(b). The inputs and the outputs in Figures 1(a) and 1(b) are the external excitation $F(t)$ and the structural response $x(t)$, respectively. The block $G(z)$ in Figure 1(a) represents the discrete transfer function in Eq. (3) for the integration algorithm, while the block k in Figure 1(b) is the linear elastic stiffness of the SDOF structure and $G'(z)$ is referred to as the open-loop transfer function for the integration algorithm.

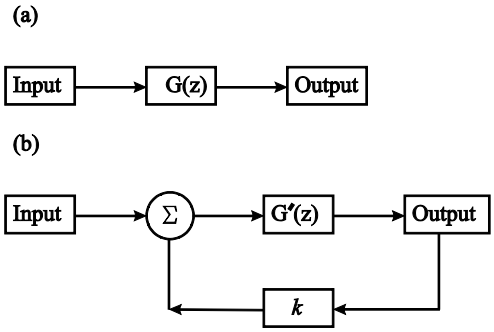

Figure 2: Block diagram representation of: (a) open loop system; and (b) closed loop system.

The relationship between the discrete transfer functions $G(z)$ and $G'(z)$ can be expressed as

$$G(z) = \frac{G'(z)}{1 + k \cdot G'(z)} \tag{6}$$

To determine the parameters for the integration algorithms defined by Eqs. (2a) and (2b), the open-loop transfer function $G'(z)$ for the Newmark method with constant average accelera-

tion is utilized in this paper, where its coefficients are tabulated in Table 2 and the discrete transfer function of $G'(z)$ can be written as

$$G'(z) = \frac{(z^2 + 2z + 1) \cdot \Delta t^2}{(4m + 2c \cdot \Delta t) \cdot z^2 - 8m \cdot z + (4m - 2c \cdot \Delta t)} \tag{7a}$$

Numerator		Denominator	
n_2	Δt^2	d_2	$4m + 2c \cdot \Delta t$
n_1	$2\Delta t^2$	d_2	$-8m$
n_0	Δt^2	d_0	$4m - 2c \cdot \Delta t$

Table 2. Coefficients of G'(z) for the Newmark method with constant average acceleration.

It can be observed that the discrete transfer function $G'(z)$ has duplicate zeros at $z = -1$. To develop an integration algorithm with numerical damping, the transfer function $G'(z)$ in Eq. (7a) is assigned to have two duplicate zeros at $z = -\lambda$, which can then be written as

$$G'(z) = \frac{(z + \lambda)^2 \cdot \Delta t^2}{(4m + 2c \cdot \Delta t) \cdot z^2 - 8m \cdot z + (4m - 2c \cdot \Delta t)} \tag{7b}$$

where λ is a positive real number and has a value between zero and one. If Eq. (7b) is used for the open-loop transfer function, the corresponding closed-loop transfer function can be derived using Eq. (6) as

$$G(z) = \frac{X(z)}{F(z)} = \frac{(z + \lambda)^2 \cdot \Delta t^2}{(4m + 2c \cdot \Delta t + k \cdot \Delta t^2) \cdot z^2 + (-8m + 2\lambda \cdot k \cdot \Delta t^2) \cdot z + (4m - 2c \cdot \Delta t + k \cdot \Delta t^2)} \tag{8a}$$

The poles of the discrete transfer function in Eq. (8a) can be derived by setting the denominator equal to zero and solving for the values of z:

$$(4m + 2c \cdot \Delta t + k \cdot \Delta t^2) \cdot z^2 + (-8m + 2\lambda \cdot k \cdot \Delta t^2) \cdot z + (4m - 2c \cdot \Delta t + k \cdot \Delta t^2) = 0 \tag{8b}$$

Assigning the poles of the closed-loop transfer function of Eq. (8b) to the transfer function $G(z)$ for the integration algorithms defined by Eqs. (2a) and (2b), and solving for α_1 and α_2 leads to

$$\alpha_1 = \frac{2m \cdot (\lambda^2 + 2\lambda + 1)}{(2\lambda^2 + 4\lambda + 2) \cdot m + (3 + 2\lambda - \lambda^2) \cdot c \cdot \Delta t + 2k \cdot \Delta t^2)} \tag{9a}$$

$$\alpha_2 = \frac{4m \cdot (\lambda + 1)}{(2\lambda^2 + 4\lambda + 2) \cdot m + (3 + 2\lambda - \lambda^2) \cdot c \cdot \Delta t + 2k \cdot \Delta t^2)} \tag{9b}$$

For different values of the parameter λ, Eqs. (9a) and (9b) lead to different sets of integration parameters α_1 and α_2, and a family of explicit integration algorithms, which will be referred to the new algorithm. It can also be derived that for the case of λ equal to 1.0, Eqs. (9a) and (9b) reduce to

$$\alpha_1 = \alpha_2 = \frac{4m}{4m + 2c \cdot \Delta t + k \cdot \Delta t^2} \tag{10}$$

Eq. (10) gives the integration parameters for the unconditionally stable explicit CR integration algorithm [10]. This indicates that the CR algorithm can be considered as a special case of the new integration algorithms.

4 STABILITY AND ACCURACY ANALYSIS

With the integration parameters defined in Eqs. (9a) and 9(b), the discrete transfer function for the new family of integration algorithms can be derived and written in the general form of Eq. (3). The coefficients are tabulated in Table 3. The stability and accuracy of the family of algorithms are then investigated using Eqs. (4) through (5b).

Numerator		Denominator	
n_2	0	d_2	$2\cdot k\cdot\Delta t^2-(\lambda+1)\cdot(\lambda-3)\cdot c\cdot\Delta t+2(\lambda+1)^2\cdot m$
n_1	$4(\lambda+1)\cdot\Delta t^2$	d_1	$4\lambda\cdot k\cdot\Delta t^2+4(\lambda^2-1)\cdot c\cdot\Delta t-4(\lambda+1)^2\cdot m$
n_0	$2(\lambda^2-1)\cdot\Delta t^2$	d_0	$2\lambda^2\cdot k\cdot\Delta t^2-(\lambda+1)\cdot(3\lambda-1)\cdot c\cdot\Delta t+2(\lambda+1)^2\cdot m$

Table 3. Coefficients of G(z) for the new algorithms.

4.1 Stability analysis for linear elastic SDOF structures

Figure 3 shows the spectral radius of the new family of integration algorithms for a linear elastic SDOF structure, where ω_n is the natural frequency of the SDOF structure. Zero viscous damping (i.e., c=0) is assumed to represent the most critical case for stability. Different values are used for the parameter λ, including λ=1.0, 0.75 and 0.5. Also presented in Figure 3 is the Newmark method with constant average acceleration. It can be observed that for selected values of λ in Figure 3, the new algorithm is stable for $\omega_n\Delta t$ up to 6.0. It can be further shown that the new algorithm is unconditional stable with λ between zero and one for any value of $\omega_n\Delta t$. Figure 3 also shows that for λ equal to 1.0, the new algorithm has the same spectral radius as the CR algorithm. This further proves that the CR algorithm is a special case of the new family of integration algorithms.

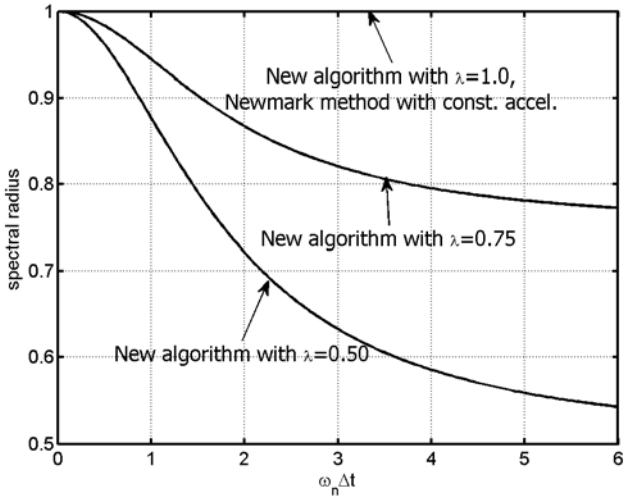

Figure 3: Spectral radius for the new family of integration algorithms.

4.2 Accuracy analysis for linear elastic SDOF structures

The accuracy of the family of new integration algorithms is analyzed using numerical damping (ND) and period elongation (PE). The SDOF structure is assumed to have zero inherent viscous damping. The equivalent damping computed from Eq. (5b) therefore represents the numerical damping introduced by the new algorithms. Cases with the values of λ equal to 1.0, 0.75 and 0.5 are considered. Figure 4 shows the numerical damping of the new algorithms, where it is compared with the Newmark method with constant average acceleration integration algorithm. The new algorithm with λ=1.0 and the Newmark method with constant average acceleration have almost zero numerical damping. When λ takes values of 0.75 and 0.5, the new algorithm is shown to introduce significant numerical damping, approaching 25% and 10% for values of $\omega_n\Delta t$ greater than 3.0, respectively. This numerical damping will help to minimize the effects of unrealistic higher mode response and the experimental errors during the structural experiments. However, Figure 4 also shows that the new algorithm introduces numerical damping for small values of $\omega_n\Delta t$ smaller than 3.0.

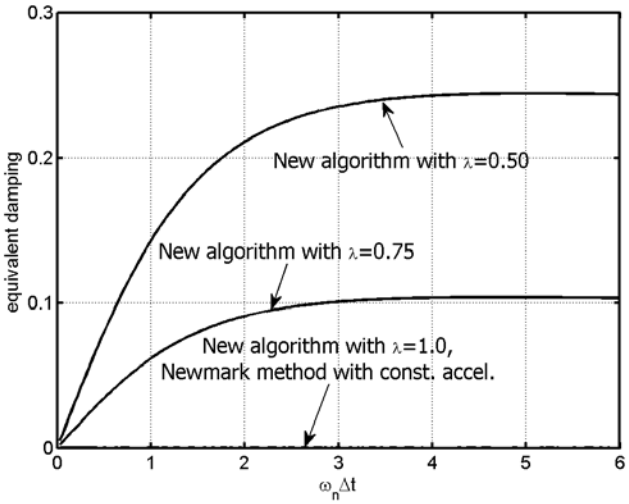

Figure 4. Numerical damping of the new algorithm.

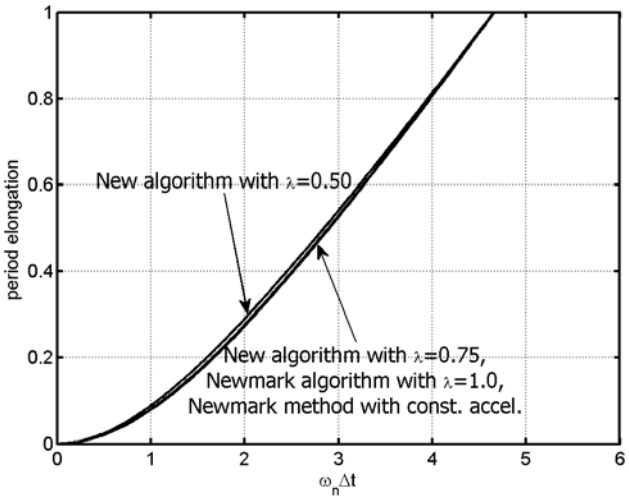

Figure 5. Period elongation of the new algorithm.

The period elongation presented in Figure 5 is observed to be almost same for the new algorithms for the various values of λ. The new algorithm with λ=1.0 is observed to be identical as that of the Newmark method with constant average acceleration. The new algorithm is shown to introduce period elongation for all three values of λ equal to 1.0, 0.75 and 0.5, but nearly identical as that of the Newmark method with constant acceleration for all cases.

4.3 Stability analysis for nonlinear SDOF structure

The above analysis indicates that the new family of explicit integration algorithms have comparable stability and accuracy properties as the Newmark method with constant average acceleration. Application of an integration algorithm for structural dynamic analysis often involves nonlinear structural behavior. Chen and Ricles [11, 12] proposed to use the discrete transfer function to analyze the stability limits of direct integration algorithms for nonlinear structural behavior. For a SDOF nonlinear structure, the equation of motion in Eq. (2) can be revised as

$$m \cdot \ddot{x}_{i+1} + c \cdot \dot{x}_{i+1} + r_{i+1} = F_{i+1} \tag{11a}$$

In Eq. (11a), r_{i+1} is the restoring force of the nonlinear SDOF structure at the $(i+1)^{\text{th}}$ time step. Eq. (11a) can be written in an incremental form as

$$m \cdot \Delta\ddot{x}_i + c \cdot \Delta\dot{x}_i + \cdot \Delta r_i = \Delta F_i \tag{11b}$$

The increments of acceleration $\Delta\ddot{x}_i$, velocity $\Delta\dot{x}_i$ and restoring force Δr_i are defined as $\Delta\ddot{x}_i = \ddot{x}_{i+1} - \ddot{x}_i$, $\Delta\dot{x}_i = \dot{x}_{i+1} - \dot{x}_i$ and $\Delta r_i = r_{i+1} - r_i$. For small values of Δt, the increment of restoring force can be approximated as $\Delta r_i = r_{i+1} - r_i = k_t \cdot \Delta x_i$ [17], where k_t is the tangent stiffness of the nonlinear SDOF structure. Using the open loop block diagram in Figure 2(b), the new integration algorithms can be represented by an open-loop transfer function G'(z) with the restoring force expressed by a varying feedback gain representing the varying stiffness [11]. The open-loop discrete transfer function can again be written in the general form in Eq. (3) and its coefficients are tabulated in Table 4.

Numerator		Denominator	
n_2	0	d_2	$2 \cdot k \cdot \Delta t^2 - (\lambda+1) \cdot (\lambda-3) \cdot c \cdot \Delta t + 2(\lambda+1)^2 \cdot m$
n_1	$4(\lambda+1) \cdot \Delta t^2$	d_1	$-4k \cdot \Delta t^2 + 4(\lambda^2-1) \cdot c \cdot \Delta t - 4(\lambda+1)^2 \cdot m$
n_0	$2(\lambda^2-1) \cdot \Delta t^2$	d_0	$2k \cdot \Delta t^2 - (\lambda+1) \cdot (3\lambda-1) \cdot c \cdot \Delta t + 2(\lambda+1)^2 \cdot m$

Table 4: Coefficients of G'(z) for the new algorithms.

The root locus approach is then used to determine the stability limit of the new family of explicit integration algorithms. Figure 6 shows a typical root locus for the open-loop transfer function with λ equal to 1.0. It can be observed that one branch of the root loci falls outside the unit circle. Therefore the new algorithm with is only stable for a finite range of stiffness values. The root locus plot crosses the unit circle at $z = -1$, and the stability limit for the improved CR algorithm can therefore be solved by substituting $z = -1$ into the denominator of the closed-loop transfer function derived from G'(z), whereby

$$\begin{aligned} &[2 \cdot k \cdot \Delta t^2 - (\lambda+1) \cdot (\lambda-3) \cdot c \cdot \Delta t + 2(\lambda+1)^2 \cdot m] \cdot z^2 - [4(k - k_t(1+\lambda) \cdot \Delta t^2 \\ &- 4(\lambda^2-1) \cdot c \cdot \Delta t + 4(\lambda+1)^2 \cdot m] \cdot z + [2(k - k_t + \lambda^2 k_t) \cdot \Delta t^2 - (\lambda+1) \cdot (3\lambda-1) \cdot c \cdot \Delta t \\ &+ 2(\lambda+1)^2 \cdot m]\big|_{z=-1} = 0 \end{aligned} \tag{12}$$

Solving Eq. (12) for k_t leads to

$$k_t \le \frac{4[-k \cdot \Delta t^2 + (\lambda^2 - 1) \cdot c \cdot \Delta t - m \cdot (\lambda + 1)^2]}{(\lambda - 3) \cdot (\lambda + 1) \Delta t^2} \tag{13a}$$

Eq. (13a) gives the stability limit for the new algorithms when applied to nonlinear SDOF structures. The stability limit in Eq. (13a) is observed to be dependent on the parameter λ as well as the structure properties (*m*, *c*, and *k*) and the integration time step *Δt*.

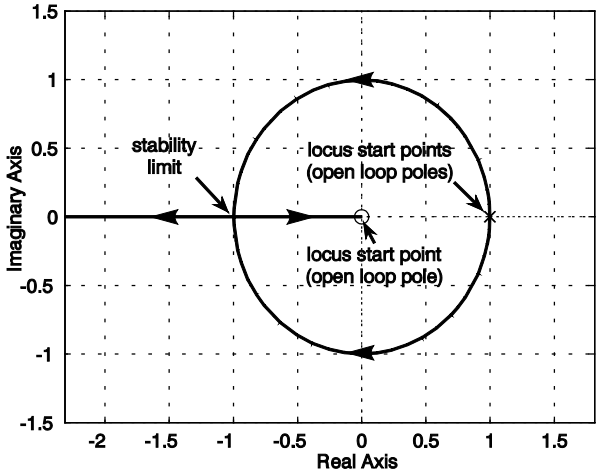

Figure 6: Typical root locus of the open loop transfer function *G'*(*z*) for the new integration algorithm (λ=1.0).

Eq. (13a) can be revised and expressed as

$$\left(\frac{k_t}{m}\right) \cdot \Delta t^2 \le \frac{4[-\omega_n^2 \Delta t^2 + (\lambda^2 - 1) \cdot 2\zeta \cdot \omega_n \Delta t - (\lambda + 1)^2]}{(\lambda - 3) \cdot (\lambda + 1)} \tag{13b}$$

where ζ is the inherent viscous damping ratio of the SDOF structure. Figure 7 shows the variation of the stability limit in Eq. (13b) with respect to the value of λ for the case of ζ=0.0. It can be observed that larger values of λ would lead to a larger stability limit.

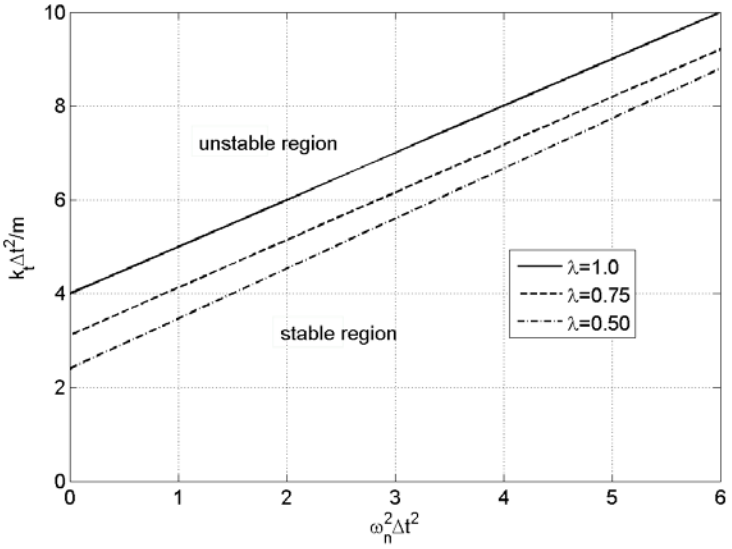

Figure 7: Stability limits for the new algorithms applied to nonlinear SDOF structure.

For the case of λ equal to one, the stability limit in Eq. (13) reduces to

$$k_t \le \frac{k \cdot \Delta t^2 + 4m}{\Delta t^2} \tag{14a}$$

Eq. (14a) is same as the stability limit for the CR algorithm applied to a nonlinear structure [11]. When the algorithm is applied to a linear elastic structure, i.e., $k_t = k$, the stability limit in Eq. (13) reduces to

$$k\Delta t^2 \le \frac{4[(\lambda^2 - 1) \cdot c \cdot \Delta t - m \cdot (\lambda + 1)^2]}{(\lambda - 3) \cdot (\lambda + 1) + 4} \tag{14b}$$

For the case of λ equal to one, the stability limit in Eq. (14b) can be further simplified as $k\Delta t^2 \le \infty$, which implies that the algorithm is stable for all values of ω_n and Δt.

5 SUMMARY AND CONCLUSIONS

This paper presents the development of a new family of unconditionally stable explicit integration algorithms with controllable numerical damping using the discrete control theory. A parameter λ is utilized to introduce and control the numerical damping for the new algorithms. Using different values of λ between zero and one results in different properties of the new algorithms. The stability of the algorithm is investigated for both linear and nonlinear structures. The new algorithms are demonstrated to be unconditionally stable for a linear elastic structure and conditionally stable for a nonlinear structure. The accuracy of the new algorithms is investigated for linear elastic structures in terms of numerical damping and period elongation. For the range of the parameter λ investigated in the present study, the new algorithm is shown to introduce small period elongation and significant numerical damping for high frequencies. This makes this new algorithms especially appealing for real-time structural testing.

REFERENCES

[1] N.M. Newmark, A Method of Computation for Structural Dynamics. *Journal of Engineering Mechanics Division* (ASCE), 85, EM3, 67-94, 1959.

[2] H.M. Hilber, T.J.R. Hughes, and R.L. Taylor, Improved Numerical Dissipation for Time Integration Algorithms in Structural Mechanics. *Earthquake Engineering and Structural Dynamics*, 5(3), 283-292, 1977.

[3] W.L. Wood, *Practical Time-Stepping Schemes*. Clarendon Press, Oxford, 1990.

[4] K. Takanashi, K. Udagawa, M. Seki, T. Okada, and H. Tanaka, Nonlinear Earthquake Response Analysis of Structures by a Computer-Actuator On-Line System. Bulletin of Earthquake Resistant Structure Research Center, University of Tokyo, Tokyo, Japan, vol. 8, 1975

[5] S.A. Mahin and P.B. Shing, Pseudodynamic Method for Seismic Testing. *Journal of Structural Engineering* (ASCE), 111(7), 1482 –1503, 1985.

[6] P.B. Shing, M.T. Vannan, and E. Cater, Implicit Time Integration for Pseudodynamic Tests. *Earthquake Engineering and Structural Dynamics*, 20, 551–576, 1991.

[7] M. Nakashima, H. Kato, and E. Takaoka, Development of Real-time Pseudo Dynamic Testing. *Earthquake Engineering and Structural Dynamics*, 21(1), 79-92, 1992.

[8] P.A. Bonnet, C.N. Lim, M.S. Williams, A. Blakeborough, S.A. Neild, D.P. Stoten, and CA. Taylor, Real-time Hybrid Experiments with Newmark Integration, MCSmd Outer-loop Control and Multi-tasking Strategies. *Earthquake Engineering. and Structural Dynamics*, 36(1), 119-141, 2007.

[9] S.Y. Chang, Explicit Pseudodynamic Algorithm with Unconditional Stability. *Journal of Engineering Mechanics* (ASCE), 128(9), 935-947, 2002.

[10] C. Chen and J.M. Ricles, Development of Direct Integration Algorithms for Structural Dynamics Using Discrete Control Theory. *Journal of Engineering Mechanics* (ASCE), 134(8), 676-683, 2008.

[11] C. Chen and J.M. Ricles, Stability Analysis of Direct Integration Algorithms Applied to Nonlinear Structural Dynamics. *Journal of Engineering Mechanics* (ASCE), 134(9), 703-711, 2008.

[12] C. Chen and J.M. Ricles, Stability Analysis of Direct Integration Algorithms Applied to MDOF Nonlinear Dynamics," *Journal of Engineering Mechanics* (ASCE), 136(4), 432-440, 2010.

[13] C. Chen, J.M. Ricles, T.M. Marullo and O. Mercan, Real-time Hybrid Testing Using the Unconditionally Stable Explicit CR Integration Algorithm. Earthquake Engineering. and Structural Dynamics, 38(1), 23-44, 2009.

[14] P.B. Shing, Development of High-Speed On-Line Substructuring Testing System at the University of Colorado. CASCADE Technical Workshop, Oxford, UK, 2002.

[15] C. Chen, J.M. Ricles, R. Sause, T.L. Karavasilis, and Y. Chae, Design and Experimental Evaluation of Steel MRF with Magneto-Rheological Dampers for Seismic Hazard Mitigation. Behavior of Steel Structures in Seismic Areas (STESSA), August 16-19, Philadelphia, PA, 2009.

[16] C. Chen, J.M. Ricles, T. Karavasilis, Y. Chae, and R. Sause, Real-Time Hybrid Simulation System for Performance Evaluation of Structures with Rate Dependent Devices Subjected to Seismic Loading. *Engineering Structures*, submitted, under review, 2010 .

[17] K. Ogata, *Discrete-Time Control Systems*, 2nd Edition, Prentice-Hall, New Jersey, 1995.

[18] A.K. Chopra, *Dynamics of Structures: Theory and Applications to Earthquake Engineering*, 2nd Edition, Prentice-Hall, New Jersey, 2001.